

## Tautomeric Fluxional Process in Metal Complexes. Insight into Cobalt(III) and Pentamethylcyclopentadienylrhodium(III) Complexes of 2-Mercaptopyrimidine Ligand

Ok-Sang Jung,\* Yong Tae Kim, Yun Ju Kim, Jung-Kyoun Chon,<sup>†</sup> and Hee K. Chae<sup>†,\*</sup>

Materials Chemistry Research Center, Korea Institute of Science and Technology, Seoul 136-791, Korea

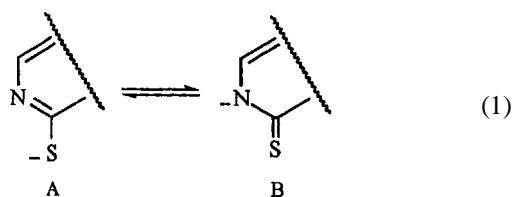
<sup>†</sup>Department of Chemistry, Hankyong University of Foreign Studies, Yongin 449-791, Korea

Received March 2, 1999

Studies have been carried out on the unusual molecular nonrigidity of  $\text{Co}^{\text{III}}(\text{PymS})_3$  and  $\text{Cp}^*\text{Rh}^{\text{III}}(\text{PymS})_2$  (PymS: 2-mercaptopyrimidine). The crystal structure of  $\text{Co}^{\text{III}}(\text{PymS})_3$  approximates to an octahedral *mer* isomer with 4-membered N-S chelating fashion. For  $\text{Cp}^*\text{Rh}^{\text{III}}(\text{PymS})_2$ , one PymS ligand bonds to the rhodium ion in an S-monodentate mode ( $\text{Rh-S}(2) = 2.366(1) \text{ \AA}$ ) while the other ligand chelates to the metal ion in an N,S-bidentate mode ( $\text{Rh-S}(1) = 2.414(1)$ ;  $\text{Rh-N}(1) = 2.103(3) \text{ \AA}$ ). Even though the conformations and configurations of both complexes are still retained in solution, an unusual nonrigidity for the protons of the PymS region is observed in the solution. The broad proton signals of  $\text{Co}^{\text{III}}(\text{PymS})_3$  exhibit a temperature-dependence in the range of  $-40 \sim 40 \text{ }^\circ\text{C}$  with a free energy of activation  $\Delta G^\ddagger = 64.49 \text{ kJ/mol}$  ( $40 \text{ }^\circ\text{C}$ ). For  $\text{Cp}^*\text{Rh}^{\text{III}}(\text{PymS})_2$ , such a fluxionality has been markedly observed in solution. This fluxional behavior can be explained in terms of "ligand tautomerism" in metal complexes containing potential tautomeric forms.

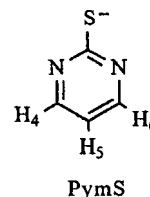
### Introduction

A series of 2-mercaptopyrimidine analogues gives rise to an extensive chemistry with both useful models for sulfur containing biomolecular bases<sup>1</sup> and structural diversity.<sup>2</sup> Their typical bonding modes include monodentate (N or S), bridging N-S, or chelate N-S with exceptionally small bite angle, where they may act as a neutral or as an anionic form. Furthermore, their anionic ligands are capable of chelating to metal ions as either thiol (A) or its tautomeric thione form (B) (eq 1).<sup>3,4</sup> The bonding fashion of the ligands can be



directed by various factors such as the basicity of the central metal, the overall charge of the complex, and medium effects.<sup>5-13</sup> Such tautomeric equilibria can be applied to deduce general structure-stability relationships,<sup>14,15</sup> quantum mechanical calculations,<sup>16</sup> molecular switches,<sup>17</sup> tautomeric catalysts,<sup>18</sup> and theories of genetic mutation.<sup>14</sup> Recently, in particular, many important biological molecules have been found to exist as tautomers in solution.

Some metal complexes of 2-mercaptopyrimidine and its analogous ligands have been structurally elucidated in the solid state. However, their solution-properties remained ambiguously until a good example on metal-mediated inter-ligand tautomerism was recently reported as a communication.<sup>19</sup> In order to extend and to clarify the unusual observation, we describe the structural properties and nonrigidity observed in new cobalt(III) and cyclopentadienyl-



rhodium(III) complexes of 2-mercaptopyrimidine (PymS) ligand that may be tautomerized and be coordinated to metal centers in a variety of modes.<sup>9</sup>

### Experimental Section

**Chemicals and Measurements.** 2-Mercaptopyrimidine (PymS), cobalt(II) chloride, and pentamethylcyclopentadienylrhodium(III) chloride were purchased from Aldrich. Chemical analyses were carried out by the Advanced Analysis Center at KIST. IR spectra were recorded on a Perkin Elmer 16F PC model FT-IR spectrometer as KBr pellets. <sup>1</sup>H and <sup>13</sup>C NMR spectra were measured on a Varian Gemini 200 or 500 (variable temperature spectra) NMR spectrometer. The chemical shifts were relative to internal Me<sub>4</sub>Si (<sup>1</sup>H and <sup>13</sup>C).

**Preparation of  $\text{Co}^{\text{III}}(\text{PymS})_3 \cdot \text{H}_2\text{Cl}_2$ .**  $\text{CoCl}_2 \cdot 6\text{H}_2\text{O}$  (0.24 g, 1 mmol) and potassium salt of PymS (0.44 g, 3.1 mmol) were combined in 30 mL of water. The mixture was stirred for 1 h at room temperature. The precipitate was filtered and dried to obtain crude solids. Recrystallization in dichloromethane gave dark brown crystals in 90% yield. IR (KBr,  $\text{cm}^{-1}$ ): 1562 (s), 1544 (s), 1428 (m), 1374 (s), 1252 (w), 1244 (w), 1170 (m), 800 (w), 754 (w). <sup>13</sup>C NMR ( $\text{Me}_2\text{NC}(\text{O})\text{H-d}_7$ , ppm): 183.93 (br), 182.69 (br, 2C), 158.94, 158.48, 158.25, 157.93, 157.55, 156.35, 115.81, 115.20, 114.69. Partial evaporation of dichloromethane molecules of the solvate

crystals resulted in erratic chemical analysis (C, H, N).

**Preparation of Cp\*Rh<sup>III</sup>(PymS)<sub>2</sub>.** To a solution of [Cp\*RhCl<sub>2</sub>]<sub>2</sub> (0.10 g, 0.16 mmol) in 10 mL methanol was added a solution of K[PymS] (0.09 g, 0.64 mmol) in 5 mL methanol. The dark red suspension was stirred for 1 day, resulting in reddish-brown solids. The product was extracted in chloroform to remove potassium chloride. Recrystallization of the crude product in a mixture of CH<sub>2</sub>Cl<sub>2</sub>/CH<sub>3</sub>CN afforded reddish-brown crystals suitable for X-ray diffraction studies in 81% yield. IR (KBr, cm<sup>-1</sup>): 1557 (s), 1528 (m), 1369 (s), 1172 (m), 796 (w), 751 (w). <sup>13</sup>C NMR (CDCl<sub>3</sub>, ppm): 8.87 (5C), 95.86 (5C), 113.04, 113.71, 154.37, 155.81, 157.12, 181.88 (2C), 184.50. Found: C, 46.80; H, 4.58; N, 12.19%. Calcd for C<sub>18</sub>H<sub>21</sub>N<sub>4</sub>S<sub>2</sub>Rh: C, 46.96; H, 4.60; N, 12.17%.

**X-ray Studies of Co<sup>III</sup>(PymS)<sub>3</sub>·H<sub>2</sub>Cl<sub>2</sub> and Cp\*Rh<sup>III</sup>(PymS)<sub>2</sub>.** Each crystal recrystallized was wedged in a Lindemann capillary with mother liquor. All X-ray data were collected on an Enraf-Nonius CAD4 automatic diffractometer with graphite-monochromated Mo Kα (λ = 0.71073 Å) at ambient temperature. Unit cell dimensions were based on 25 well-centered reflections by using a least-square procedure. During the data collection, three standard reflections monitored every hour did not show any significant intensity variation. All data were collected with the ω/2θ scan mode. The data were corrected for Lorentz and polarization effects. Absorption effects were corrected by the empirical psi-scan method. The structure was solved by Patterson method (SHELXS-86), and were refined by full-matrix least squares techniques (SHELXL-93).<sup>20</sup> All non-hydrogen atoms were refined anisotropically and hydrogen atoms were added at calculated positions. For Co(PymS)<sub>3</sub>·CH<sub>2</sub>Cl<sub>2</sub>, non-hydrogen atoms of solvate dichloromethane molecules were refined isotropically. The crystal parameters and procedural information corresponding to data collection and structure refinement are given in Table 1.

## Results

**Co<sup>III</sup>(PymS)<sub>3</sub>.** The variable temperature <sup>1</sup>H NMR spectra of Co(PymS)<sub>3</sub> in CDCl<sub>3</sub> are shown in Figure 1. Complicated resonances (1 : 2 : 2 : 1 : 1 : 1 : 1) in the range of 6.70–8.70 ppm come from three non-equivalent PymS ligands within the complex, indicating that *mer* isomer is retained without any geometrical isomerism in the solution. Among the signals, in particular, two broad resonances at 8.42 ppm and 7.48 ppm in the 2 : 1 integral ratio are now interesting. The two signals are characterized as the protons of ring carbons adjacent to coordinated nitrogen atoms of the PymS units (Their assignment along with other peaks was achieved via <sup>1</sup>H/<sup>13</sup>C COSY NMR of PyS analogue).<sup>19</sup> The high field shift of one proton (7.48 ppm) relative to the other two protons (8.42 ppm) was explained via a π-electron effect: in the *mer* configuration one of the three protons lies perpendicularly above the plane of another PymS ligand and shifts upfield due to the magnetic anisotropy. The two peaks are broad even though the basic structure is retained in solution. The peaks exhibit a temperature-dependence in the range of

**Table 1.** Crystal Data and Structure Refinement for Co<sup>III</sup>(PymS)<sub>3</sub>·H<sub>2</sub>Cl<sub>2</sub> and Cp\*Rh<sup>III</sup>(PymS)<sub>2</sub>

Formula (crystallographic)	C <sub>24</sub> H <sub>18</sub> N <sub>12</sub> S <sub>6</sub> Co <sub>2</sub> ·2CH <sub>2</sub> Cl <sub>2</sub>	C <sub>18</sub> H <sub>21</sub> N <sub>4</sub> S <sub>2</sub> Rh
Formula weight	982.84	460.42
Temperature, K	293(2)	293(2)
Space group	P <sub>c</sub> (No. 7)	P2 <sub>1</sub> /n
a, Å	12.403(7)	10.242(1)
b, Å	10.266(2)	10.920(2)
c, Å	14.588(3)	17.260(4)
β, deg	98.73(2)	98.99(2)
V, Å <sup>3</sup>	1836(1)	1906.8(6)
Z	2	4
d <sub>cal</sub> , Mg/m <sup>3</sup>	1.727	1.604
Absorption coeff., mm <sup>-1</sup>	1.577	1.123
F(000)	960	936
Crystal size, mm	0.20×0.20×0.40	0.40×0.40×0.45
Theta range, deg	1.41–24.95	2.17–24.96
Index ranges	h, k, ±1	h, k, ±1
Reflections collected	2637	2708
Independent reflections	2637 [R(int) = 0.0000]	2566 [R(int) = 0.0181]
Refined parameters	421	226
Goodness-of-fit on F <sup>2</sup>	1.881	1.083
Final R indices	R1 = 0.0803, wR2 = 0.2173	R1 = 0.0307, wR2 = 0.0775
[I > 2σ(I)]		
R indices (all data)	R1 = 0.0809, wR2 = 0.2184	R1 = 0.0312, wR2 = 0.0779
Largest diff. peak & hole, eÅ <sup>-3</sup>	0.587 and -1.016	0.624 and -0.306

$$R1 = \frac{\sum ||F_o| - |F_c||}{\sum |F_o|}, wR2 = \frac{\sum w(F_o^2 - F_c^2)^2 / F_o^4}{\sum w(F_o^2 + (aP)^2 + bP)}^{1/2}, \text{ where } w = 1 / \{ \sigma^2 F_o^2 + (aP)^2 + bP \} \text{ with } P = \{ \text{Max}(F_o^2, 0) + 2F_c^2 \} / 3$$

-40~40 °C (Figure 1). The peak at 8.42 ppm has a coalescent temperature at 40 °C with a free energy of activation ΔG<sup>‡</sup> =

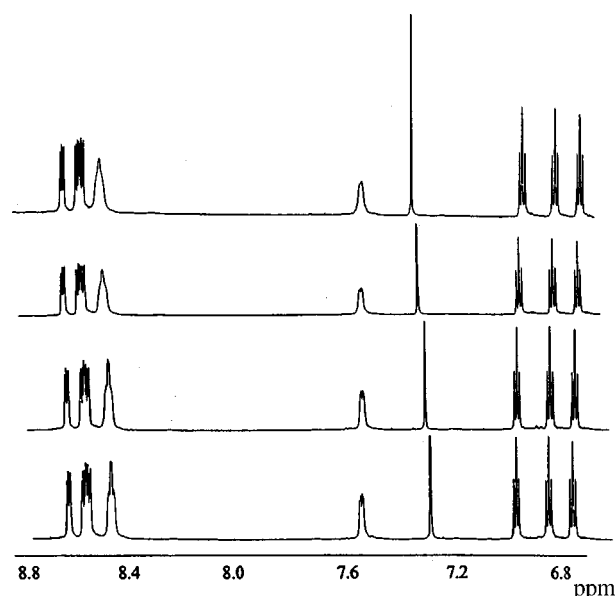


**Figure 1.** Variable-temperature <sup>1</sup>H NMR (CDCl<sub>3</sub>) of Co(PymS)<sub>3</sub> ppm. Peak at 7.28 ppm indicates chloroform. From top to bottom: 40 °C, 10 °C, -15 °C, and -40 °C.

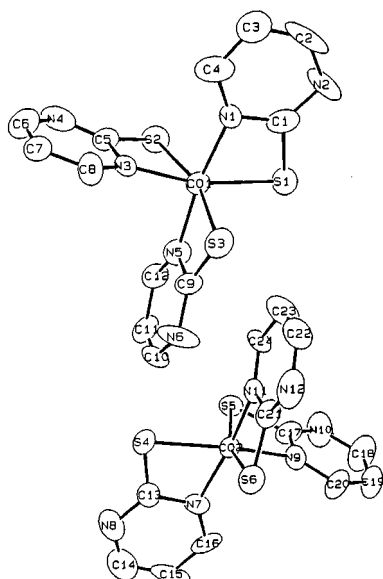


**Figure 2.** Crystal structure (50% probability ellipsoids) of  $\text{Co}(\text{PymS})_3 \cdot \text{H}_2\text{Cl}_2$ . Solvate dichloromethane molecules and hydrogen atoms are omitted for clarity.

64.49 kJ/mol,<sup>21</sup> and begins to separate into two chemical shifts. Each chemical shift finally appears as a doublet (*via* coupling with a neighboring proton) as the temperature is decreased down to  $-40^\circ\text{C}$ . The peak at 7.48 ppm has similar behavior that appears as a doublet at  $-40^\circ\text{C}$ .

The molecular structure of  $\text{Co}(\text{PymS})_3 \cdot \text{CH}_2\text{Cl}_2$  is depicted in Figure 2, and the relevant bond lengths and angles are listed in Table 2. There are two independent molecules in the

**Table 2.** Bond Lengths (Å) and Angles ( $^\circ$ ) for  $\text{Co}^{\text{III}}(\text{PymS})_3 \cdot \text{CH}_2\text{Cl}_2$  and  $\text{Cp}^*\text{Rh}^{\text{III}}(\text{PymS})_2$

Co(1)-N(1)	1.90(2)	Rh-C(9)	2.174(4)
Co(1)-S(1)	2.289(5)	Rh-N(1)	2.104(3)
C(1)-S(1)	1.73(2)	Rh-S(1)	2.414(1)
C(5)-S(2)	1.69(2)	Rh-S(2)	2.366(1)
C(9)-S(3)	1.72(2)	C(1)-S(1)	1.730(4)
C(13)-S(4)	1.70(2)	C(5)-S(2)	1.738(4)
C(17)-S(5)	1.75(2)		
C(21)-S(6)	1.74(2)		
N(1)-Co(1)-N(3)	94.9(6)	S(1)-Rh-S(2)	88.12(4)
N(1)-Co(1)-N(5)	170.0(7)	S(1)-Rh-N(1)	67.8(1)
N(3)-Co(1)-N(5)	93.0(7)	S(2)-Rh-N(1)	90.75(9)
N(1)-Co(1)-S(1)	73.3(5)	N(1)-C(1)-S(1)	109.7(3)
N(3)-Co(1)-S(1)	165.6(4)	N(3)-C(5)-S(2)	119.6(3)
N(5)-Co(1)-S(1)	99.7(5)	Rh-S(1)-C(1)	80.5(2)
N(1)-Co(1)-S(2)	92.4(5)	Rh-N(1)-C(1)	102.0(3)
N(3)-Co(1)-S(2)	71.8(4)	Rh-S(2)-C(5)	105.9(2)
N(5)-Co(1)-S(2)	95.8(5)		
N(1)-Co(1)-S(3)	100.1(5)		
N(3)-Co(1)-S(3)	96.7(5)		
N(5)-Co(1)-S(3)	72.9(5)		
S(2)-Co(1)-S(3)	163.7(2)		
S(1)-Co(1)-S(3)	93.6(2)		
S(1)-Co(1)-S(2)	100.0(2)		

asymmetric region of the monoclinic unit cell. Because of the limited "typical 4-membered bite angle" of the PymS ligand, the local geometry around the cobalt atom is highly distorted ( $\text{S-Co-N}$ ,  $71.4(5)\sim 73.3(5)^\circ$ ) from regular octahedron. The lengths of Co-S and Co-N bonds are similar to the corresponding distances of well-known compounds.<sup>22</sup> Only the *mer* isomer was confirmed, and thus the overall structure is similar to that of the  $\text{Co}(\text{PyS})_3$  ( $\text{PyS} = 2\text{-mercaptopyridine}$ ).<sup>23</sup> For Co1 molecule, the C(1)-S(1) (1.73(2) Å) of a PymS ligand is much longer than the corresponding bond (1.692(2) Å) of PySH ligand<sup>12</sup> (the crystal structure of PymSH is not available) that exists as a thione tautomer in the solid state, whereas the C(5)-S(2) (1.69(2) Å) is very close to that of PySH. The C(9)-S(3) length (1.71(2) Å) is a median value of the two limited lengths. For molecule 2, the C(13)-S(4), 1.703(2) Å approximates to a thione form whereas the bond lengths of C(17)-S(5), 1.75(2) Å and C(21)-S(6), 1.74(2) Å have a significant amount of thiol. This observation suggests that the PymS ligands within the compound are functioning as mixed tautomeric forms within the standard deviation.

**$\text{Cp}^*\text{Rh}^{\text{III}}(\text{PymS})_2$ .** The bridge-cleavage reaction of the dimer  $[\text{Cp}^*\text{Rh}(\text{III})\text{Cl}_2]_2$  with potassium salt of PymS smoothly yielded  $\text{Cp}^*\text{Rh}^{\text{III}}(\text{PymS})_2$ . X-ray characterization was performed to reveal the exact structure depicted in Figure 3, and its relevant bond lengths and angles were listed in Table 2. The structure consists of discrete molecules, with a formally six-coordinate Rh(III) center. The PymS ligands adopt two coordination fashions: one PymS ligand bonds to the rhodium ion in an S-monodentate mode ( $\text{Rh-S}(2) = 2.366(1)$  Å) while the other chelates to the metal atom in an N,S-bidentate mode ( $\text{Rh-S}(1) = 2.414(1)$ ;  $\text{Rh-N}(1) = 2.103(3)$  Å). The local geometry around the rhodium atom is distorted due to the "typical 4-membered bite angle" with the bite angle of  $\text{S}(1)\text{-Rh-N}(1)$  ( $67.8(1)^\circ$ ). The C(1)-S(1) (1.730(4) Å) and C(5)-S(2) (1.738(4) Å) are much longer

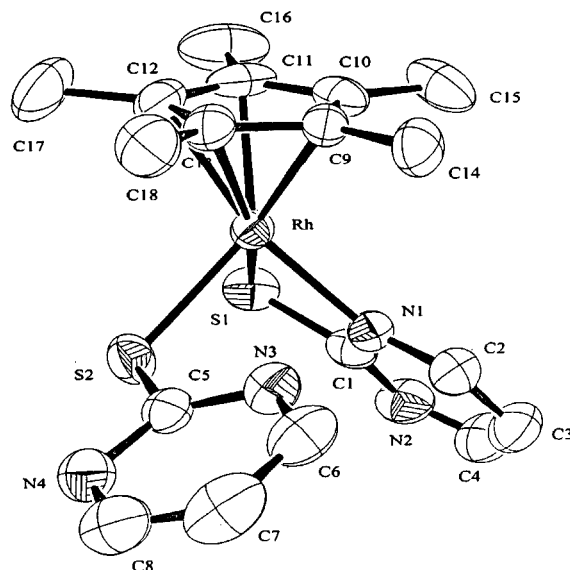


**Figure 3.** Crystal structure (50% probability ellipsoids) of  $\text{Cp}^*\text{Rh}^{\text{III}}(\text{PymS})_2$ . Hydrogen atoms are omitted for clarity.

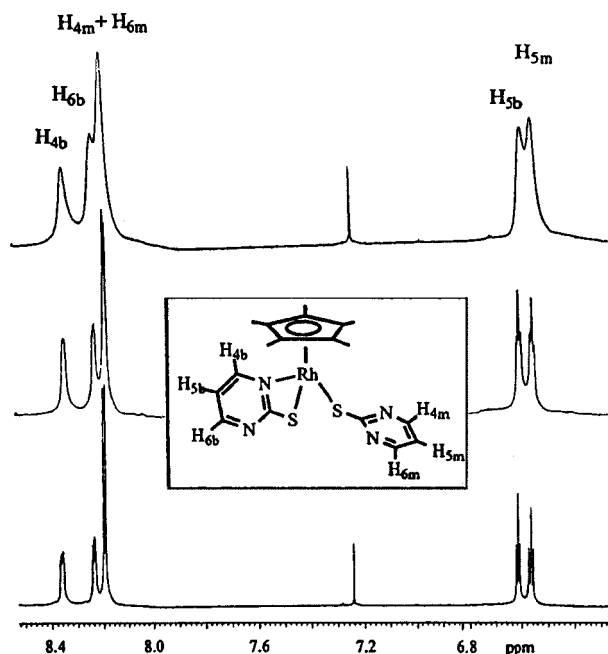


**Figure 4.** Variable-temperature  $^1\text{H}$  NMR ( $\text{CDCl}_3$ ) of  $\text{Cp}^*\text{Rh}^{\text{III}}(\text{PymS})_2$ . Peak at 7.28 ppm indicates chloroform. Top (30  $^\circ\text{C}$ ), middle (15  $^\circ\text{C}$ ), and bottom (0  $^\circ\text{C}$ ).

than the corresponding bond (1.692(2)  $\text{\AA}$ ) of free  $\text{PySH}$  ligand,<sup>12</sup> indicating that both  $\text{PymS}$  groups have a significant amount of thiol in the solid state.

$^1\text{H}$  NMR spectrum of the  $\text{PymS}$  region consists of five broad peaks at 8.34, 8.24, 8.18, 6.58, and 6.54 ppm in a 1 : 1 : 2 : 1 : 1 integral ratio at 30  $^\circ\text{C}$ , which is consistent with the X-ray structure in the solid state. The five resonances could be assigned as  $\text{H}_{4b}$ ,  $\text{H}_{6b}$ ,  $\text{H}_{4m} + \text{H}_{6m}$ , and  $\text{H}_{5b}$ ,  $\text{H}_{5m}$  protons (b = bidentate; m = monodentate), respectively. Great difference between  $\text{H}_{4b}$  and  $\text{H}_{4m}$  chemical shifts adjacent to nitrogen atom seems to originate from the coexistence of bidentate and monodentate  $\text{PymS}$  groups. Variable temperature NMR spectra were monitored to solve the reason of the broad resonances. The broad peaks exhibit a marked temperature-dependence in the range of 0–30  $^\circ\text{C}$  (Figure 4). Cooling the sample to 15  $^\circ\text{C}$  separates the broad chemical shifts, and at 0  $^\circ\text{C}$  the static spectrum with clear coupling constants was observed, demonstrating that  $\text{Cp}^*\text{Rh}^{\text{III}}(\text{PymS})_2$  in the cold solution is locked into the crystal structure. Solvent-dependent  $^1\text{H}$  NMR spectra are designated in Figure 5, disclosing that the proton signals are greatly affected by solvents.

### Discussion

The broad peaks of the present  $\text{Co}(\text{PymS})_3$  are slightly shifted downfield relative to those of  $\text{Co}(\text{PyS})_3$ . Furthermore, the coalescent temperature of  $\text{Co}(\text{PymS})_3$  is higher than that of the  $\text{Co}(\text{PyS})_3$ .<sup>19</sup> The subtle difference between the two compounds seems to originate from the structural properties of the ligands. The similar studies on  $\text{Co}(\text{PySO})_3$  ( $\text{PySO} = 2\text{-mercaptopyridine N-oxide}$ ) were also carried out,

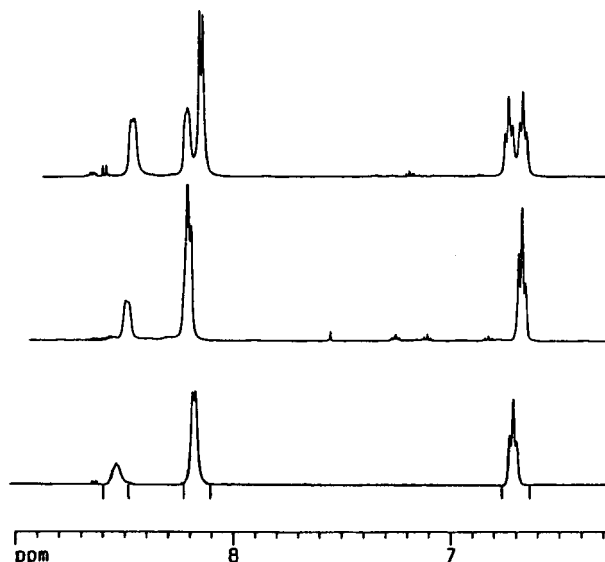
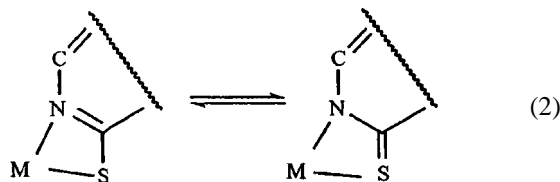


**Figure 5.** Solvent-dependent  $^1\text{H}$  NMR spectra ( $\text{Me}_2\text{SO-d}_6$  (top),  $\text{CD}_3\text{CN}$  (middle), and  $\text{CD}_3\text{OD}$  (bottom)) of the  $\text{PymS}$  region in  $\text{Cp}^*\text{Rh}^{\text{III}}(\text{PymS})_2$ .

but  $\text{fac-Co}(\text{PySO})_3$  (which was found to be *fac*-isomer<sup>24,25</sup> in contrast to *mer-Co}(\text{PymS})\_3) containing 5-membered N–O chelate rings does not exhibit the unique fluxional process in the same temperature range:  $^1\text{H}$  NMR spectrum (8.30 (d), 7.42 (d), 7.09 (t), and 6.83 (t) ppm) exhibits a simple rigid structure. Thus, the fluxionality is strongly dependent upon the structure of the potential tautomeric ligand including the angle strain of chelate as well as donating atoms. Such a phenomenon is very sensitive to solvents such as water, dimethyl sulfoxide or dimethylformamide. For instance, addition of water into the organic solution results in decreasing the rate of the fluxional motion, presumably due to the solvation effects of polar water molecules. The everlasting presence of two resonances at 8.42 ppm and 7.48 ppm indicates that an isomerism between *fac* and *mer* isomers do not occur in the temperature range.*

For  $\text{Cp}^*\text{Rh}^{\text{III}}(\text{PymS})_2$ , the absence of coalescence of the two  $\text{H}_4$  peaks in the temperature range of  $-5\sim 40$   $^\circ\text{C}$  rules out the possibility of a ligand-scrambling process via a trigonal twist and a chelate ring opening between the monodentate and bidentate ligands. In contrast,  $\text{Rh}(\text{PyS})_3$  does not reveal the tautomerism.<sup>8</sup> Furthermore, the steric effect of  $\text{Cp}^*$  seems to obstruct the rotational conformer of the monodentate  $\text{PymS}$  ligand: such a rigidity in the molecule is easily visualized by examining a space-filling view (Figure 3). The fluxional behaviors may be delicately tuned by solvents used ( $\text{Me}_2\text{SO-d}_6$ ,  $\text{CD}_3\text{CN}$ ,  $\text{CD}_3\text{OD}$ ) (Figure 5). Though both the chemical shifts and the tautomerism exhibit a marked solvent dependence, the appearance of two resonances corresponding to  $\text{H}_{4b}$  and  $\text{H}_{4m}$  precludes the ligand-scrambling process between the monodentate and bidentate ligands even in all the solvents. The strong solvent effects may be useful to specific solvent recognition. Considering above all data, the unusual fluxionality should be induced by the pliable  $\text{PymS}$  ligands bonded to the metal(III) ion. The dynamical

process that is possible for the present system is "thiol/thione tautomerism in metal complexes" around room temperature while the molecular skeleton is retained. The tautomeric equilibria of the ligand can be extended to some organometallic complexes (eq 2). Assuming above results, the crucial



factors of the tautomerism may be induced. Potential tautomeric ligands such as PyS and PymS are essential for the tautomerism. The unique tautomerism may be affected by the central metals, the chelate rings, the local geometry of metal atoms, the donating atom of ligands, the solvents, the coligands. Further studies on other metal complexes including solvent and ligand effects will provide more detailed information about the origin and availability of the molecular motion observed in a wide range of chemical and biological fields.

In conclusion, the cobalt(III) and rhodium(III) complexes of 2-mercaptopyrimidine are unusual examples that exhibit electronically pliability between mixed tautomeric ligands. This unique molecular nonrigidity is subtly dependent on various conditions such as the central metal, the chelate ring, the local geometry of metal atom, the donating atom of ligands, coligands, and the solvents. Our successive observation may provide a clue to understand the molecular fluxional motion occurring in molecules such as thiouracil and thiocytosine that can be tautomerized.

**Acknowledgment.** This research was supported financially by the Ministry of Science and Technology in Korea. We would like to thank Dr. Sang-gi Lee for variable temperature  $^1\text{H}$  NMR spectra and valuable discussion.

**Supporting Information Available.** X-ray data are available from OSJ (Tel: (02) 958-5086, Fax: (02) 958-5089, e-mail: oksjung@kist.re.kr).

### References

- Povey, D. C.; Smith, G. W.; Lobana, T. S.; Bhatia, P. K. *J. Crystallogr. Spectroscopic Res.* **1991**, *21*, 9.
- Rosenfield, S. G.; Swedberg, S. A.; Arora, S. K.; Mascharak, P. K. *Inorg. Chem.* **1986**, *25*, 2109.
- Jia, G.; Puddephatt, R. J.; Vital, J. J. *Polyhedron* **1992**, *11*, 2009.
- Reynolds, J. G.; Sendlinger, S. C.; Murray, A. M.; Huffman, J. C.; Christou, G. *Inorg. Chem.* **1995**, *34*, 5745.
- Jung, O.-S.; Park, S. H.; Lee, Y.-A.; Cho, Y.; Kim, K. M.; Lee, S.; Chae, H. K.; Sohn, Y. S. *Inorg. Chem.* **1996**, *35*, 6899.
- Deeming, A. J.; Meah, M. N. N.; Dawes, H. M.; Hursthouse, M. B. *J. Organomet. Chem.* **1986**, *299*, C25.
- Rosenfield, S. G.; Berends, H. P.; Gelmini, L.; Stephan, D. W.; Mascharak, P. K. *Inorg. Chem.* **1987**, *26*, 2792.
- Deeming, A. J.; Hardcastle, K. I.; Meah, M. N.; Bates, P. A.; Dawes, H. M.; Hursthouse, M. B. *J. Chem. Soc., Dalton Trans.* **1988**, 227.
- Yap, G. P. A.; Jensen, C. M. *Inorg. Chem.* **1992**, *31*, 4823.
- Cookson, P. D.; Tiekink, E. R. T. *J. Chem. Soc., Dalton Trans.* **1993**, 259.
- Pramanik, A.; Bag, N.; Chakravorty, A. *Inorg. Chem.* **1993**, *32*, 811.
- Perez-Torrente, J. J.; Casado, M. A.; Ciriano, M. A.; Lahoz, F. J.; Oro, L. A. *Inorg. Chem.* **1996**, *35*, 1782.
- Deeming, A. J.; Meah, M. N. *Inorg. Chim. Acta* **1986**, *117*, L13.
- Beak, P.; Fry, Jr., F. S.; Lee, J.; Steele, F. *J. Am. Chem. Soc.* **1976**, *98*, 171.
- Ozeki, H.; Cockett, M. C. R.; Okuyama, K.; Takahashi, M.; Kimura, K. *J. Phys. Chem.* **1995**, *99*, 8608.
- Wang, J.; Boyd, R. J. *J. Phys. Chem.* **1996**, *100*, 16141.
- Jung, O.-S.; Pierpont, C. G. *J. Am. Chem. Soc.* **1994**, *116*, 1127.
- Rony, P.; Neff, R. O. *J. Am. Chem. Soc.* **1973**, *95*, 2896.
- Jung, O.-S.; Kim, Y. T.; Lee, Y.-A.; Chae, H. K. *Bull. Korean Chem. Soc.* **1998**, *19*, 286.
- (a) Sheldrick, G. M. SHELXS-86: A Program for Structure Determination; University of Göttingen: Germany, 1986. (b) Sheldrick, G. M. SHELXL-93: A Program for Structure Refinement; University of Göttingen: Germany, 1993.
- $\Delta G^\ddagger$  values were calculated from  $k_c = \pi \cdot \Delta v/2$ ;  $\Delta G^\ddagger = 2.3RT_c(10.32 + \log T_c/k_c)$ ; see for the equation, Lambert, J. B.; Shurvell, H. F.; Vervit, L.; Cooks, R. G.; Stout, G. H. *Organic Structural Analysis*; Macmillan Publishing Co: New York, 1976; p 116.
- Cartwright, B. A.; Goodgame, D. M. L.; Jeeves, I.; Langguth, P. O.; Skapski, A. C. *Inorg. Chim. Acta* **1977**, *24*, L45.
- Constable, E. C.; Palmer, C. A.; Tocher, D. A. *Inorg. Chim. Acta* **1990**, *176*, 57.
- Hu, Y.-H.; Weng, L.-H.; Huang, L.-R.; Chen, X.-T.; Wu, D.-X.; Kang, B.-S. *Acta Cryst.* **1991**, *C47*, 2655.
- Hu, Y.-H.; Kang, B.-S.; Chen, X.-T.; Huang, L.-R. *Acta Cryst.* **1991**, *C47*, 2655.